Contemporary Mathematics
https://ojs.wiserpub.com/index.php/CM/

Research Article

Computing the Neighbourhood Multiple Topological Indices of Dendritic Graphs

Tumiso Kekana[1], Kazeem Olalekan Aremu[1,2*], Maggie Aphane[1]

[1]Department of Mathematics and Applied Mathematics, Sefako Makgatho Health Sciences University, Ga-Rankuwa, P.O Box 60, Pretoria, 0204, South Africa
[2]Department of Mathematics, Usmanu Danfodiyo University, Sokoto, P.M.B 2346, Sokoto State, Nigeria
E-mail: aremu.kazeem@udusok.edu.ng

Received: 5 November 2024; **Revised:** 16 December 2024; **Accepted:** 19 December 2024

Abstract: In this article, we extend the traditional multiple degree-based topological indices (TIs) to neighborhood multiple degree-based TIs with the aim of studying the branching and generation of three distinct dendrimers namely, poly (propyl ether imine) (PETIM), zinc porphyrin, and porphyrin. We defined and computed six existing neighborhood versions of multiple degree-based TIs for the dendrimers. The computational analysis revealed that our TIs display exponential or linear growth as the dendrimer generations increase. Our findings reveal that the extended TIs such as the second Zagreb index ($\Gamma_M M_2(\mathfrak{G})$) and forgotten index ($\Gamma_M F(\mathfrak{G})$) effectively capture the highest structural complexity, showing rapid exponential growth with each generation. In contrast, TIs; atom bond connectivity index ($\Gamma_M ABC(\mathfrak{G})$) and Randíc index ($\Gamma_M R(\mathfrak{G})$) exhibit more moderate or linear growth, indicating their focus on more localized structural characteristics. These results contribute to a broader understanding of the dendrimer's structural complexity and connectivity highlighting their potential in drug delivery applications. The research also reveals critical insights on the neighborhood multiple degree-based TI's role as an efficient molecular descriptor that can characterize connectivity patterns of complex graphs. The analytical results have a further implication on the quantitative structure-property relationship (QSPR) modeling of these dendrimers.

***Keywords*:** neighborhood multiple topological indices, porphyrin dendrimer, zinc porphyrin dendrimer, PETIM dendrimer

MSC: 65L05, 34K06, 34K28

1. Introduction

Dendrimers are nanoparticles with diameters ranging from 1 to 100 nm, and they are synthesized macromolecules or polymers that play a significant role in chemical research. Their highly branching, tree-like structure, where each generation of branching adds new layers or branches to the central molecule in a gradual and repeating process, gives them unique properties and versatility. Dendrimers were first synthesized in 1978 by the German chemist Fritz Vögtle [1] and have since found applications in chemistry, biology, and nanosciences. Due to their unique structure and properties, dendrimers present significant opportunities for designing innovative materials, drug delivery systems, and nanoscale devices [2]. Ethirajan et al. [3] highlighted the significance of porphyrin dendrimers in photodynamic therapy and

DOI: https://doi.org/10.37256/cm.6220256027

nanodevices, attributing their importance to their unique capability to transfer excitation energy when exposed to light. Their versatility is particularly evident in drug delivery, where they enhance drug solubility, bioavailability, and targeting precision. The foundational principles of modern chemical graph theory (CGT) are credited to the innovative work of mathematicians Arthur Cayley (1821-1895) and James Sylvester (1814-1897). In their attempt to represent chemical structures through mathematical concepts, they established that there is an isomorphism between chemical structures and mathematical graphs [4]. A fundamental tool in CGT is the use of topological indices (TIs), which are numerical values derived from the properties of chemical graphs. TIs are generally classified into four categories: distance-based, entropy-based, spectral-based, and degree-based TIs. These TIs capture important structural information about molecules and can be used to predict various chemical and physical properties. These TIs enable dimensionality reduction, allowing for the exploration of structure-property relationships in a more manageable and interpretable manner [5].

The concept of TIs dates back to 1947 when Harold Wiener introduced the Wiener index to study molecular branching. Wiener's work demonstrated a strong correlation between the boiling points of alkane molecules and their corresponding Wiener index values [6]. Building on this foundation, two degree-based graph invariants-the first and second Zagreb indices-were introduced in the 1970s and have since become key tools in CGT (see Gutman [7]). These indices are widely used to characterize molecular structures, capturing information about their complexity and connectivity. The first and second Zagreb indices for a graph $\mathfrak{G}$ are defined as follows:

$$M_1(\mathfrak{G}) = \sum_{v \in V(\mathfrak{G})} d_v^2 = \sum_{uv \in E(\mathfrak{G})} (d_u + d_v),$$

$$M_2(\mathfrak{G}) = \sum_{uv \in E(\mathfrak{G})} (d_u d_v),$$

where $\mathfrak{G} = (V, E)$ is a graph with vertex set V and edge set E. Here, d_u and d_v represent the degrees of vertices u and v, respectively. The degree d_u of a vertex $u \in V$ is defined as the number of edges incident to u.

The same study also showcased the impact of the sum of cubes of vertex degrees in a molecular graph. However, the specific TI associated with this observation was not further explored and remained largely forgotten. Subsequently, Furtula and Gutman conducted an investigation into this "forgotten TI" and demonstrated its significant improvement in relevance compared to the first Zagreb index in physicochemical applications. Their research revealed that both the first Zagreb index and the forgotten index exhibit strong predictive capabilities for entropy and acetic factors of Alkanes, with correlation coefficients surpassing 0.95 [8]. The forgotten TI can be computed using the following formula:

$$F(\mathfrak{G}) = \sum_{u \in V(\mathfrak{G})} d_v^3 = \sum_{uv \in E(\mathfrak{G})} d_u^2 + d_v^2.$$

In 1975, Randić [9] introduced a TI that computes the degrees of edges in a molecular graph, in his article titled "On characterization of molecular branching". This index, widely known as the Randić index or the Connectivity index is certainly the most widely applied index in chemistry and pharmacology, in particular for designing quantitative structure-property and structure-activity relations. This index is given by

$$R(\mathfrak{G}) = \sum_{uv \in E(\mathfrak{G})} \frac{1}{\sqrt{d_u d_v}}.$$

Additional degree-based TIs include the atom-bond connectivity (ABC) index, the geometric-arithmetic (GA) index, and their variants (see [10–17]). In 2018, Gao et al. [18] introduced new variants of the ABC and GA indices, these

variant paved way for the multiple degree-based TIs. These TIs were computed for three grid structures: octagonal, hexagonal, and square grids. Zaman et al. analyzed various degree-based irregularity TIs for three types of dendrimers: the first kind ($D_1[n]$), the third kind (D_3n) across generations 1 to 3 with three growth stages, and the tetrathiafulvalene dendrimer ($TD_2[n]$) [19]. In another study, Zaman et al. [20] provided a comprehensive analysis of degree-based TIs for dominating David derived networks (DDDN), assessing their utility and performance in honeycomb networks. Liaqat et al. [21] recently extended the misbalance prodeg index from crisp to fuzzy graphs, where vertices and edges have varying membership values. They established bounds for this index across various graph classes, including paths, cycles, complete, bipartite, and star graphs. Similarly, Noureena et al. [22] addressed the problem of identifying tricyclic graphs of fixed order that maximize the atom-bond sum-connectivity (ABS) index, a degree-based TI. They characterized the graphs with the largest ABS index among connected tricyclic graphs of order $n \geq 5$, building on prior work in this area (see [23–25] for similar works).

Recently, researchers have focused on developing TIs based on the neighborhood degrees of vertices. The neighborhood of a vertex u, denoted by $N(\mathfrak{G})_u$, is the set of all vertices v directly connected to u. The neighborhood sum degree of u is defined as the sum of the degrees of its neighboring vertices and is expressed as:

$$\lambda_u = \sum_{v \in N(\mathfrak{G})_u} d_v.$$

Mondal et al. [26] introduced the concept of neighborhood sum degree-based TIs, which extend classical TIs by incorporating the degrees of neighboring vertices into the computation. Their work explored variations such as the neighborhood second Zagreb index, neighborhood forgotten index, modified neighborhood forgotten index, and neighborhood hyper Zagreb index, each designed to characterize molecular structures in greater detail. These indices are defined as follows for a graph $\mathfrak{G}$:

$$M_N(\mathfrak{G}) = \sum_{uv \in E(\mathfrak{G})} (\lambda_u \lambda_v),$$

$$F_N(\mathfrak{G}) = \sum_{u \in V(\mathfrak{G})} (\lambda_u)^3,$$

$$F_N^*(\mathfrak{G}) = \sum_{uv \in E(\mathfrak{G})} \left[(\lambda_v)^2 + (\lambda_u)^2\right], \quad \text{and}$$

$$HM_N(\mathfrak{G}) = \sum_{uv \in E(\mathfrak{G})} (\lambda_v + \lambda_u)^2.$$

In their application to quantitative structure-property relationship (QSPR) analysis, Mondal et al. [26] observed that the newly introduced neighborhood TIs outperformed their degree-based TIs counterparts when applied to model the physicochemical properties of octane isomers. Following this, Mondal et al. [27] extended this concept by introducing neighborhood variations of several degree-based TIs, including the second modified Zagreb index, general Randić index, harmonic index, and inverse sum index. These TIs were derived from the neighborhood M-polynomials of crystallographic structures. Abubakar et al. [28] studied the bounds of the neighborhood geometric arithmetic index and the neighborhood atom bond connectivity index, investigating their graph theoretic properties on various graphs such as star graphs, cycle graphs, and complete graphs. Ullah et al. computed novel neighborhood-based molecular descriptors for two carbon nanosheets and derived corresponding formulas for these descriptors [29] (see [30–32] for the applications of neighborhood degree-based TIs in drug property modeling using machine learning).

This study focuses on characterizing the branching and generation of dendrimers through the computation of neighborhood multiple degree-based TIs. These indices present an important contribution to study of TIs, extending beyond traditional degree-based TIs, multiple degree-based TIs, and neighborhood sum degree-based TIs. While degree-based TIs rely solely on the degrees of each vertex, and neighborhood sum TIs incorporate the sum of neighboring vertex degrees, the proposed neighborhood multiple TIs introduce a framework by considering the multiplicative product of the degrees of neighboring vertices for a given vertex. This allows the TIs to capture the global structural properties of chemical graphs, which will be particularly useful for structures with complex branching, particularly dendrimers and nanotubes. Using neighborhood multiple TIs, this work explicitly traces dendrimers' complex branching patterns and growth mechanisms from generation to generation.

Finally, this study applies the proposed neighborhood multiple TIs to analyze three specific dendritic graph types: poly propyl ether imine (PETIM), zinc porphyrin (DPZ_n), and porphyrin (D_nP_n) dendrimers. These graphs have been previously studied using degree-based and neighborhood sum degree-based TIs, but this approach provides new perspectives and extends the scope of these analyses. By leveraging the enhanced sensitivity of neighborhood multiple TIs, the work uncovers new insights into the structural and generative properties of these dendrimers. Building on the foundational work of Gao et al. [18] and Mondal et al. [26, 27], researchers [33–43] have demonstrated the utility of diverse TIs in characterizing the structural complexities of dendrimers, including zinc porphyrin, porphyrin, Poly(amidoamine) (PAMAM), nanostar, fractal, and Cayley tree types. These studies establish critical connections between dendrimer structures and their physicochemical properties. However, the full potential of neighborhood sum degree-based TIs, particularly their multiplicative extensions, remains unexplored. This work bridges that gap by defining and computing six neighborhood multiple degree-based TIs, demonstrating their applicability and significance in analyzing dendrimer growth and branching patterns.

2. Preliminaries

Consider a graph $\mathfrak{G} = (V, E)$. The following definitions represent adaptations of the multiple degree-based TIs originally introduced by Gao et al. in their seminal work [18].

Definition 1 The neighborhood multiple degree function $\xi_u = \prod_{v \in N(\mathfrak{G})_u} d_v$ is defined as the product of the degrees of all vertices v in the neighborhood of vertex u.

Definition 2 In a graph $\mathfrak{H}$, the neighborhood multiple-edge partition sets for all edges $uv \in E(\mathfrak{H})$ are defined by the pairs (ξ_u, ξ_v).

Definition 3 [18] Let $\mathfrak{G}$ be a chemical graph.

(i) The neighborhood multiple Atom-bond connectivity index is defined by

$$\Gamma_M ABC(\mathfrak{G}) = \sum_{uv \in E(\mathfrak{G})} \sqrt{\frac{\xi_u + \xi_v - 2}{\xi_u \xi_v}}. \tag{1}$$

(ii) The neighborhood multiple Geometric arithmetic index is defined by

$$\Gamma_M GA(\mathfrak{G}) = \sum_{uv \in E(\mathfrak{G})} \frac{2\sqrt{\xi_u \xi_v}}{\xi_u + \xi_v}. \tag{2}$$

(iii) The neighborhood multiple first Zagreb index is defined by

$$\Gamma_M M_1(\mathfrak{G}) = \sum_{uv \in E(\mathfrak{G})} (\xi_u + \xi_v). \tag{3}$$

(iv) The neighborhood multiple second Zagreb index is defined by

$$\Gamma_M M_2(\mathfrak{G}) = \sum_{uv \in E(\mathfrak{G})} (\xi_u \xi_v). \tag{4}$$

(v) The neighborhood multiple Randić index is defined by

$$\Gamma_M R(\mathfrak{G}) = \sum_{uv \in E(\mathfrak{G})} \frac{1}{\sqrt{\xi_u \xi_v}}. \tag{5}$$

(vi) The neighborhood multiple Forgotten index is defined by

$$\Gamma_M F(\mathfrak{G}) = \sum_{uv \in E(\mathfrak{G})} (\xi_u^2 + \xi_v^2). \tag{6}$$

Remark 1 The six neighborhood multiple TIs in Definition 3 are neighborhood multiple degree-based descriptors that capture diverse structural properties of chemical graphs. These TIs are interconnected as they are all derived from the neighborhood multiple degree functions ξ_u and ξ_v associated with the vertices u and v of each edge $uv \in E(\mathfrak{G})$. They emphasize additive (3), multiplicative (4), ratio-based (1), (2), inverse (5), and extreme (6) degree contributions.

The subsequent lemmas are used to determine the number of vertices and edges of the arbitrary graph $\mathfrak{G}$.

Lemma 1 (Handshaking Lemma [41]) Consider the graph $\mathfrak{G}$. Then

$$\frac{\sum_{v \in V(\mathfrak{G})} d_v}{2} = |E|.$$

In this context, $V(\mathfrak{G})$ represents the vertex set of $\mathfrak{G}$, d_v stands for the degree of a vertex v, and $|E|$ indicates the total number of edges in the graph $\mathfrak{G}$.

Lemma 2 (Tree Lemma [41]) For a tree graph $\mathfrak{G}$, the formula for determining the total number of vertices is expressed as $|E| + 1$, where $|E|$ represents the total number of edges. That is

$$|V| = |E| + 1.$$

Remark 2 The Handshaking Lemma is an important tool utilized in this research as it ensures that the total degree sum across all vertices equals twice the number of edges. For dendrimers, this validates the branching structure and consistency of the graph's structure. While the Tree Lemma validates the tree-like structures of the dendrimers by ensuring that the dendrimer's edge count is consistent with its acyclic nature, confirming it is a valid tree.

3. Methodology

This study computes neighborhood multiple degree-based TIs for poly propyl ether imine (PETIM), zinc porphyrin (DPZ_n), and porphyrin (D_nP_n) dendrimers. We begin by presenting the molecular structures of the dendrimers, followed by partitioning the neighborhood multiple degrees of the end-vertices of each edge. In Figure 1, we present the flowchart for the computational process of our methodology.

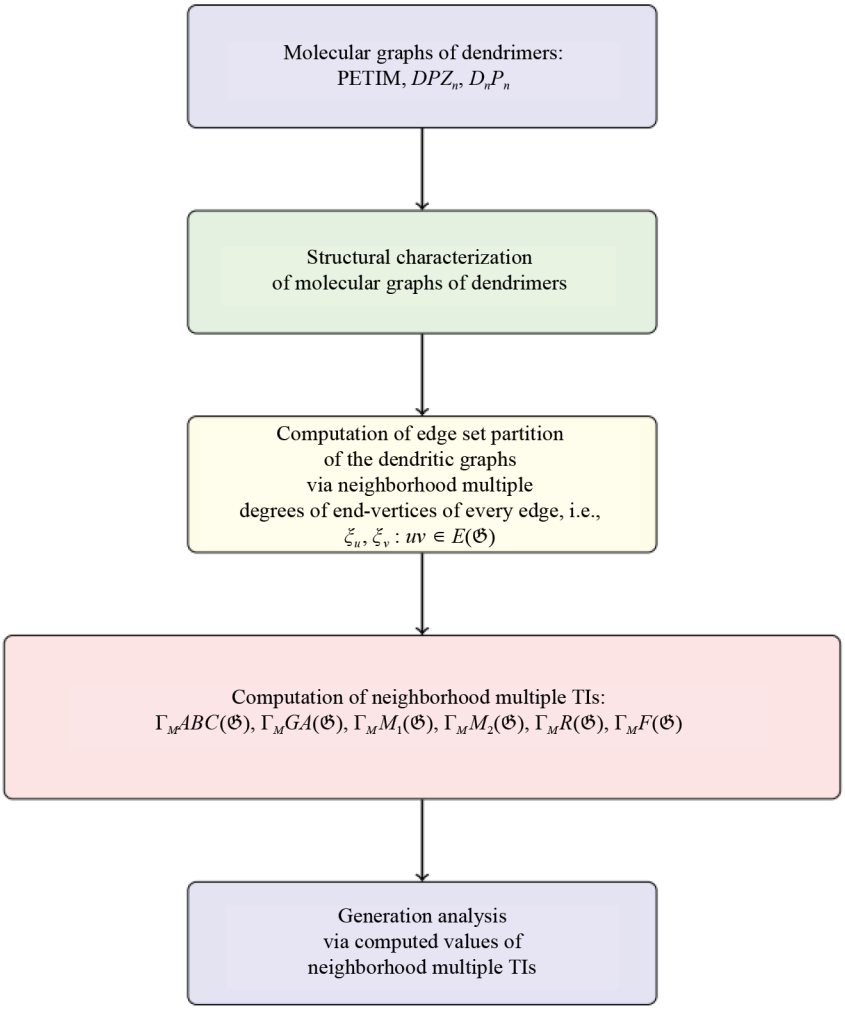

Figure 1. Flowchart illustrating the computational steps of generation analysis via neighborhood multiple TIs

4. Main results

4.1 *Neighborhood multiple degree-based TIs of poly (propyl) ether imine*

The PETIM dendrimer of generation n with $n \geq 1$ (see Figure 2) begins its three-dimensional growth from an oxygen atom at its core, with branches attached to each hydrogen in the tertiary position. These branching points are termed "generation" points, and each successive generation is separated by an eight-bond spacer.

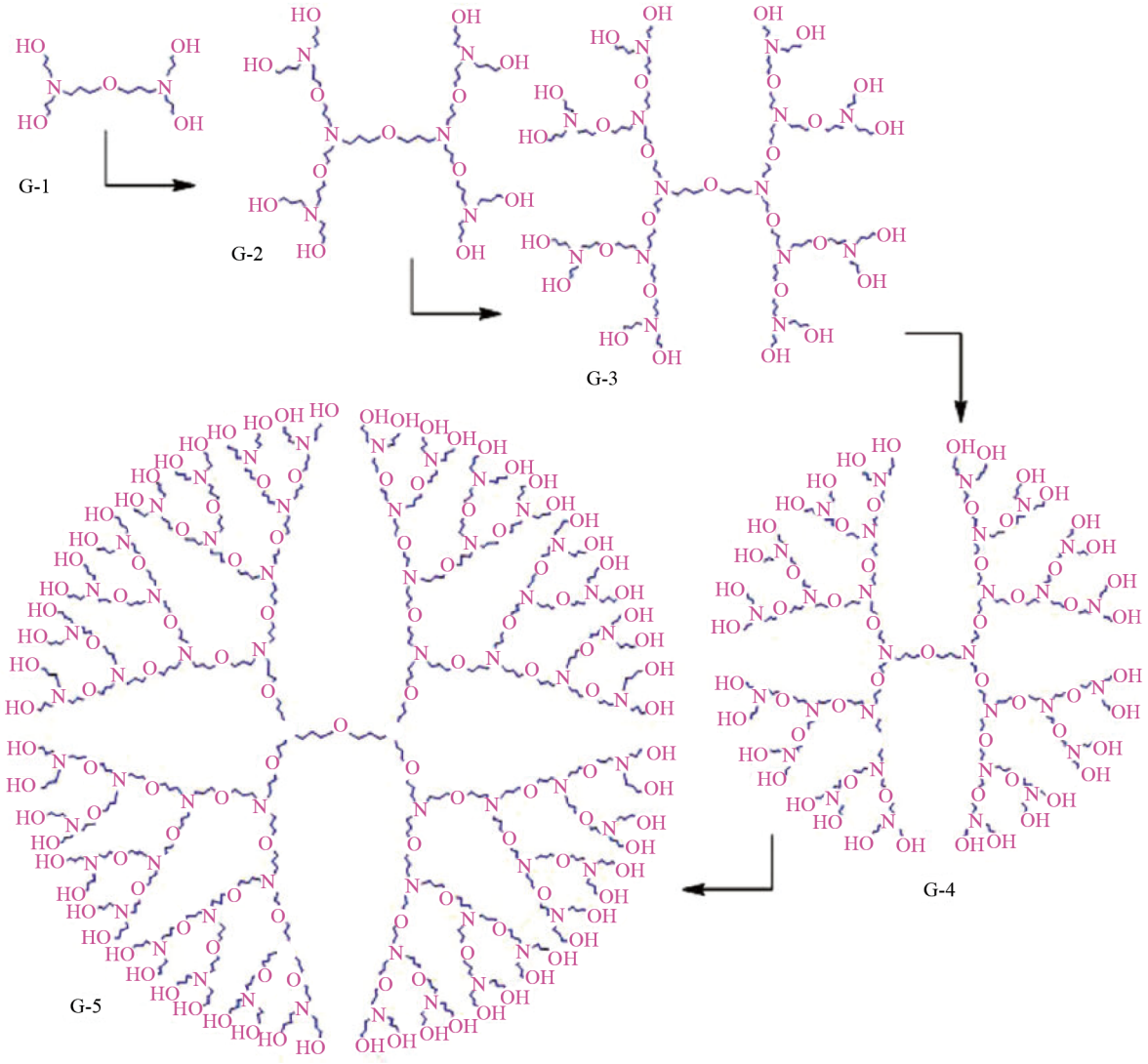

Figure 2. *n*th growth molecular graph of PETIM dendrimer [44]

To compute the structural properties of the PETIM dendrimer, we start by examining the molecular graph $\mathfrak{H}$ of the dendrimer in the following manner:

(i) The central core of $\mathfrak{H}$ contains 8 edges.

(ii) Each of the 4 branches in $\mathfrak{H}$ has $2^{n+1} \times 3 - 8$ edges, as derived in Lemma 3.

(iii) Thus, the total number of edges in $\mathfrak{H}$ is:

$$|E(\mathfrak{H})| = 4 \times (2^{n+1} \times 3 - 8) + 8 = 24 \times 2^n - 24. \tag{7}$$

Since $\mathfrak{H}$ is a tree, the total number of vertices $|V(\mathfrak{H})|$ is given by:

$$|V(\mathfrak{H})| = 24 \times 2^n - 23, \tag{8}$$

as established using Lemma 2.

Next, we determine the number of vertices with specific neighborhood multiple degrees using Definition 1. Then, we obtain that: the number of vertices with neighborhood multiple degrees of 2 is

$$\xi_2 = 2^{n+2}, \tag{9}$$

the number of vertices with neighborhood multiple degrees of 6 is

$$\xi_6 = 3 \times \left(\sum_{k=0}^{n} 2^k \right) = 3 \times 2^{n+1} - 6, \tag{10}$$

the number of vertices with neighborhood multiple degrees of 8 is

$$\xi_8 = 4 \times \left(\sum_{k=0}^{n-2} 2^k \right) + 2 = 2^{n+1} - 2, \tag{11}$$

and the remaining vertices with neighborhood multiple degrees of 4 are given by

$$\xi_4 = |V(\mathfrak{H})| - \xi_2 - \xi_6 - \xi_8 = 6 \times 2^{n+1} - 15. \tag{12}$$

Lemma 3 Let $\mathfrak{G}$ be a PETIM dendrimer with 4 branches. Then each branch has a total number of $2^{n+1} \times 3 - 8$ edges.

Proof. Take the molecular graph of PETIM dendrimer. As illustrated in (refer Figure 2), then

$$8 \times \left(\sum_{k=0}^{n-2} 2^k \right) + 4 \times 2^{n-1} = 8 \times \left(2^0 + 2^1 + 2^2 + \ldots + 2^{n-2} \right) + 4 \times 2^{n-1}$$

$$= 8 \times \left(2^{n-1} - 1 \right) + 4 \times 2^{n-1}$$

$$= 2^{n+1} \times 3 - 8.$$

□

Now we present the partitioning of the neighborhood multiple degrees of the end vertices for each edge of PETIM, using Definition 2, along with the corresponding number of edges.

Theorem 1 Let $\mathfrak{G}$ be a molecular graph of PETIM dendrimer. Then

(i) $\Gamma_M ABC(\mathfrak{G}) = 2^n \times 14.191 - 13.812$.

(ii) $\Gamma_M GA(\mathfrak{G}) = 2^{n+3} \times 2.985 - 23.817$.

(iii) $\Gamma_M M_1(\mathfrak{G}) = 2^{n+1} \times 114 - 240$.

(iv) $\Gamma_M M_2(\mathfrak{G}) = 2^n \times 584 - 624$.

(v) $\Gamma_M R(\mathfrak{G}) = 2^{n-1} \times 11.595 - 5.0907$.

(vi) $\Gamma_M F(\mathfrak{G}) = 2^{n+2} \times 306 - 4 \times 324$.

Table 1. Edge set partition of the PETIM dendrimer via neighborhood degrees of end-vertices of every edge

$\xi_u, \xi_v : uv \in E(\mathfrak{G})$	No. of edges
(2, 2)	2^{n+1}
(2, 4)	2^{n+1}
(4, 6)	$3\times 2^{n+1}-6$
(6, 8)	$3\times 2^{n+1}-6$
(4, 4)	$4\times 2^{n+1}-12$

Proof. Consider the molecular graph of PETIM dendrimer. As shown from Table 1 the vertex set $V(G)$ is partitioned into five sets according to multiple degrees of neighbors of end-vertices of every edge.

(i) From (1), we get

$$\Gamma_M ABC(\mathfrak{G}) = 2^{n+1}\sqrt{\frac{2+2-2}{2\times 2}} + 2^{n+1}\sqrt{\frac{2+4-2}{2\times 4}} + (4\times 2^{n+1}-12)\sqrt{\frac{4+4-2}{4\times 4}}$$

$$+ (3\times 2^{n+1}-6)\sqrt{\frac{6+4-2}{6\times 4}} + (3\times 2^{n+1}-6)\sqrt{\frac{6+8-2}{6\times 8}}. \tag{13}$$

Simplifying (13) further, we obtain

$$\Gamma_M ABC(\mathfrak{G}) = 2^n \times 14.191 - 13.812. \tag{14}$$

(ii) Derived from the equation (2), we obtain

$$\Gamma_M GA(\mathfrak{G}) = 2^{n+1}\frac{2\sqrt{2\times 2}}{2+2} + 2^{n+1}\frac{2\sqrt{2\times 4}}{2+4} + (4\times 2^{n+1}-12)\frac{2\sqrt{4\times 4}}{4+4}$$

$$+ (3\times 2^{n+1}-6)\frac{2\sqrt{6\times 4}}{6+4} + (3\times 2^{n+1}-6)\frac{2\sqrt{6\times 8}}{6+8}. \tag{15}$$

After simplifying (15) further, we obtain

$$\Gamma_M GA(\mathfrak{G}) = 2^{n+3} \times 2.985 - 23.817. \tag{16}$$

(iii) From (3), we get

$$\Gamma_M M_1(\mathfrak{G}) = 2^{n+1}(2+2) + 2^{n+1}(2+4) + (4\times 2^{n+1} - 12)(4+4)$$

$$+ (3\times 2^{n+1} - 6)(6+4) + (3\times 2^{n+1} - 6)(6+8) \tag{17}$$

$$= 2^{n+1}\times 114 - 240. \tag{18}$$

(iv) From (4), we get

$$\Gamma_M M_2(\mathfrak{G}) = 2^{n+1}(2\times 2) + 2^{n+1}(2\times 4) + (4\times 2^{n+1} - 12)(4\times 4)$$

$$+ (3\times 2^{n+1} - 6)(6\times 4) + (3\times 2^{n+1} - 6)(6\times 8) \tag{19}$$

$$= 2^{n}\times 584 - 624. \tag{20}$$

(v) From (5), we get

$$\Gamma_M R(\mathfrak{G}) = 2^{n+1}\frac{1}{\sqrt{2\times 2}} + 2^{n+1}\frac{1}{\sqrt{2\times 4}} + (4\times 2^{n+1} - 12)\frac{1}{\sqrt{4\times 4}}$$

$$+ (3\times 2^{n+1} - 6)\frac{1}{\sqrt{6\times 4}} + (3\times 2^{n+1} - 6)\frac{1}{\sqrt{6\times 8}}. \tag{21}$$

After simplifying (21) further, we obtain

$$\Gamma_M R(\mathfrak{G}) = 2^{n-1}\times 11.595 - 5.0907. \tag{22}$$

(vi) From (6), we get

$$\Gamma_M F(\mathfrak{G}) = 2^{n+1}(2^2+2^2) + 2^{n+1}(2^2+4^2) + (4\times 2^{n+1} - 12)(4^2+4^2)$$

$$+ (3\times 2^{n+1} - 6)(6^2+4^2) + (3\times 2^{n+1} - 6)(6^2+8^2). \tag{23}$$

After simplifying (23) further, we get

$$\Gamma_M F(\mathfrak{G}) = 2^{n+2}\times 306 - 4\times 324. \tag{24}$$

□

4.2 *Neighborhood multiple degree-based TIs of zinc porphyrin dendrimer*

The dendrimer DPZ_n of generation n, where $n \geq 1$, is depicted in Figure 3. The molecular graph $\mathfrak{H}$ of DPZ_n consists of a central core with 49 vertices and four identical branches. To compute the TIs of the dendrimer DPZ_n, we start by analyzing the molecular graph $\mathfrak{H}$ of DPZ_n:

(i) The central core of $\mathfrak{H}$ contains 49 vertices.

(ii) Each of the four branches in $\mathfrak{H}$ has $7 \times 2^{n+1} - 14$ vertices, as shown in Lemma 4.

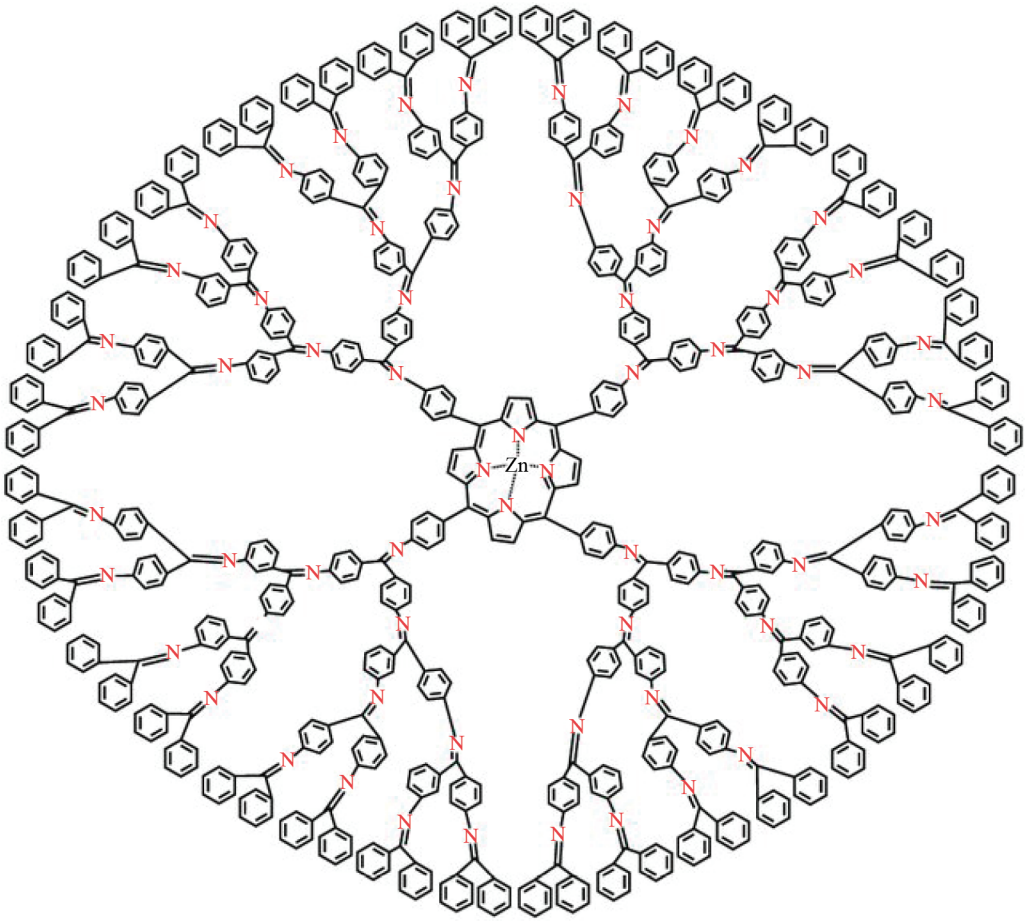

Figure 3. nth growth molecular graph of DPZ_n dendrimer [41]

Then, we determine the number of vertices with specific neighborhood multiple degrees by applying Definition 1. So we get that: the number of vertices with neighborhood multiple degrees of 9 and 18 is

$$\xi_{9,\,18} = 2^n - 1, \tag{25}$$

the number of vertices with neighborhood multiple degrees of 12 is

$$\xi_{12} = 2 \times \left(\sum_{k=0}^{n} 2^k \right) = 2^{n+1} - 2, \tag{26}$$

the number of vertices with neighborhood multiple degrees of 6 is

$$\xi_6 = 6 \times 2^{n-1}, \tag{27}$$

the number of vertices with neighborhood multiple degrees of 8 is

$$\xi_8 = 14, \tag{28}$$

and the remaining vertices with neighborhood multiple degrees of 4 are given by

$$\xi_4 = (14 \times 2^n - 14) - (2^n - 1) - (2^n - 1) - (2^{n+1} - 2) - (6 \times 2^{n-1}) - 14 = 2^n \times 7 - 24. \tag{29}$$

Thus, the total number of vertices $|V(\mathfrak{H})|$ in the molecular graph DPZ_n is:

$$|V(\mathfrak{H})| = 4 \times \left[(2^n - 1) + (2^n - 1) + (2^{n+1} - 2) + (6 \times 2^{n-1}) + (7 \times 2^n - 24) + 24\right] + 49, \tag{30}$$

which simplifies to:

$$|V(\mathfrak{H})| = 28 \times 2^{n+1} - 7. \tag{31}$$

Furthermore, the number of vertices with a degree of 2 is

$$d_2 = 20 \times 2^{n+1} - 12, \tag{32}$$

the number of vertices with a degree of 3 is

$$d_3 = 8 \times 2^{n+1} + 4, \tag{33}$$

and there is one vertex d_4 with a degree of 4.

Finally, the total number of edges $|E(\mathfrak{H})|$ in the molecular graph DPZ_n is:

$$|E(\mathfrak{H})| = 32 \times 2^{n+1} - 4, \tag{34}$$

as derived in Lemma 1.

Lemma 4 Let $\mathfrak{G}$ be a DPZ_n dendrimer with 4 branches. Then each branch has a total number of $7 \times 2^{n+1} - 14$ vertices.

Proof. Consider a molecular graph of DPN_Z dendrimer. As it shown from (refer Figure 3), then

$$14 \times \left(\sum_{k=0}^{n-1} 2^k \right) = 14 \times \left(2^0 + 2^1 + 2^2 + \ldots + 2^{n-1} \right)$$

$$= 7 \times 2 \left(2^n - 1 \right)$$

$$= 7 \times 2^{n+1} - 14.$$

□

Next, the neighborhood multiple degrees of the end vertices for each edge are partitioned according to Definition 2, and the corresponding edge counts are presented in the Table 2 below.

Table 2. Edge set partition of the DPZ_n dendrimer via neighborhood multiple degrees of end-vertices of every edge

$\xi_u, \xi_v : uv \in E(\mathfrak{G})$	No. of edges
(4, 4)	2^{n+3}
(4, 6)	8
(6, 6)	$4 \times 2^{n+2} - 12$
(6, 8)	$2^{n+3} - 12$
(6, 12)	$4 \times 2^{n+2} - 12$
(6, 18)	8
(8, 9)	2^{n+2}
(9, 12)	4
(9, 18)	$2^{n+2} - 4$
(12, 18)	$2^{n+3} - 8$
(12, 27)	4
(18, 27)	8
(18, 36)	8
(36, 81)	4

Theorem 2 Let $\mathfrak{G}$ be a molecular graph of DPZ_n dendrimer, then
(i) $\Gamma_M ABC(\mathfrak{G}) = 2^n \times 31.151 - 5.733$.
(ii) $\Gamma_M GA(\mathfrak{G}) = 2^{n+3} \times 7.825 - 5.309$.
(iii) $\Gamma_M M_1(\mathfrak{G}) = 2^n \times 1{,}072 + 680$.
(iv) $\Gamma_M M_2(\mathfrak{G}) = 2^n \times 4{,}904 + 19{,}272$.
(v) $\Gamma_M R(\mathfrak{G}) = 2^{n+3} \times 1.022 - 2.243$.
(vi) $\Gamma_M F(\mathfrak{G}) = 2^n \times 11{,}032 + 55{,}232$.
Proof. From Table 2, we prove for the following:
(i) From (1), we get

$$\Gamma_M ABC(\mathfrak{G}) = 2^{n+3}\sqrt{\frac{4+4-2}{4\times 4}} + 8\sqrt{\frac{4+6-2}{4\times 6}} + (4\times 2^{n+2}-12)\sqrt{\frac{6+6-2}{6\times 6}} + (2^{n+3}-12)\sqrt{\frac{6+8-2}{6\times 8}}$$

$$+ (4\times 2^{n+2}-12)\sqrt{\frac{6+12-2}{6\times 12}} + 8\sqrt{\frac{6+18-2}{6\times 18}} + 2^{n+2}\sqrt{\frac{8+9-2}{8\times 9}} + 4\sqrt{\frac{9+12-2}{9\times 12}}$$

$$+ (2^{n+2}-4)\sqrt{\frac{9+18-2}{9\times 18}} + (2^{n+3}-8)\sqrt{\frac{12+18-2}{12\times 18}} + 4\sqrt{\frac{12+27-2}{12\times 27}}$$

$$+ 8\sqrt{\frac{18+27-2}{18\times 27}} + 8\sqrt{\frac{18+36-2}{18\times 36}} + 4\sqrt{\frac{36+81-2}{36\times 81}}. \tag{35}$$

After simplifying (35) further, we get

$$\Gamma_M ABC(\mathfrak{G}) = 2^n \times 31.151 - 5.733. \tag{36}$$

□

(ii) Derived from the equation (1), we obtain

$$\Gamma_M GA(\mathfrak{G}) = 2^{n+3}\frac{2\sqrt{4\times 4}}{4+4} + 8\frac{2\sqrt{4\times 6}}{4+6} + 2^{n+2}\frac{2\sqrt{8\times 9}}{8+9} + 4\frac{2\sqrt{9\times 12}}{9+12} + (4\times 2^{n+2}-12)\frac{2\sqrt{6\times 6}}{6+6}$$

$$+ (2^{n+3}-12)\frac{2\sqrt{6\times 8}}{6+8} + (4\times 2^{n+2}-12)\frac{2\sqrt{6\times 12}}{6+12} + 8\frac{2\sqrt{6\times 18}}{6+18} + (2^{n+2}-4)\frac{2\sqrt{9\times 18}}{9+18}$$

$$+ (2^{n+3}-8)\frac{2\sqrt{12\times 18}}{12+18} + 4\frac{2\sqrt{12\times 27}}{12+27} + 8\frac{2\sqrt{18\times 27}}{18+27} + 8\frac{2\sqrt{18\times 36}}{18+36} + 4\frac{2\sqrt{36\times 81}}{36+81}$$

$$= 2^{n+3}\times 7.825 - 5.309. \tag{37}$$

(iii) From (3), we get

$$\Gamma_M M_1(\mathfrak{G}) = 2^{n+3}(4+4) + 8(4+6)$$

$$+ (4\times 2^{n+2}-12)(6+6) + (2^{n+3}-12)(6+8) + (4\times 2^{n+2}-12)(6+12) + 8(6+18)$$

$$+ 4\times 2^n(8+9) + 4(9+12) + (2^{n+2}-4)(9+18) + (8\times 2^n-8)(12+18)$$

$$+ 4(12+27) + 8(18+27) + 8(18+36) + 4(36+81). \tag{38}$$

After simplifying (38) further, we get

$$\Gamma_M M_1(\mathfrak{G}) = 2^n \times 1{,}072 + 680. \tag{39}$$

(iv) From (4), we get

$$\begin{aligned}\Gamma_M M_2(\mathfrak{G}) = {} & 2^{n+3}(4\times 4) + 8(4\times 6) + (4\times 2^{n+2} - 12)(6\times 6) + (2^{n+3} - 12)(6\times 8) \\ & + (4\times 2^{n+2} - 12)(6\times 12) + 8(6\times 18) + 4\times 2^n(8\times 9) + 4(9\times 12) \\ & + (2^{n+2} - 4)(9\times 18) + (2^{n+3} - 8)(12\times 18) + 4(12\times 27) \\ & + 8(18\times 27) + 8(18\times 36) + 4(36\times 81).\end{aligned} \tag{40}$$

After simplifying (40) further, we find

$$\Gamma_M M_2(\mathfrak{G}) = 2^n \times 4{,}904 - 19{,}272. \tag{41}$$

(v) From (5), we get

$$\begin{aligned}\Gamma_M R(\mathfrak{G}) = {} & 2^{n+3}\frac{1}{\sqrt{4\times 4}} + 8\frac{1}{\sqrt{4\times 6}} + (4\times 2^{n+2} - 12)\frac{1}{\sqrt{6\times 6}} + (4\times 2^{n+2} - 12)\frac{1}{\sqrt{6\times 12}} \\ & + (8\times 2^n - 12)\frac{1}{\sqrt{6\times 8}} + 8\frac{1}{\sqrt{6\times 18}} + 42^{n+2}\frac{1}{\sqrt{8\times 9}} + 4\frac{1}{\sqrt{9\times 12}} \\ & + (2^{n+2} - 4)\frac{1}{\sqrt{9\times 18}} + (2^{n+3} - 8)\frac{1}{\sqrt{12\times 18}} + 4\frac{1}{\sqrt{12\times 27}} \\ & + 8\frac{1}{\sqrt{18\times 27}} + 8\frac{1}{\sqrt{18\times 36}} + 4\frac{1}{\sqrt{36\times 81}}.\end{aligned} \tag{42}$$

After simplifying (42) further, we obtain

$$\Gamma_M R(\mathfrak{G}) = 2^{n+3} \times 1.022 - 2.243. \tag{43}$$

(vi) Derived from the equation (6), we obtain

$$\Gamma_M M_1(\mathfrak{G}) = 2^{n+3}(4^2+4^2)+8(4^2+6^2)+(4\times 2^{n+2}-12)(6^2+6^2)+(2^{n+3}-12)(6^2+8^2)$$

$$+(16\times 2^n-12)(6^2+12^2)+8(6^2+18^2)+2^{n+2}(8^2+9^2)+4(9^2+12^2)+(2^{n+2}-4)(9^2+18^2)$$

$$+(2^{n+3}-8)(12^2+18^2)+4(12^2+27^2)+8(18^2+27^2)$$

$$+8(18^2+36^2)+4(36^2+81^2). \tag{44}$$

After simplifying (44) further, we get

$$\Gamma_M F(\mathfrak{G}) = 2^n \times 11{,}032 - 55{,}232. \tag{45}$$

4.3 *Neighborhood multiple degree-based TIs of porphyrin dendrimer*

We examine the third molecular graph, the porphyrin dendrimer (D_nP_n) of generation n, where $n = 2^m$ and $m \geq 2$, as illustrated in Figure 4. The molecular graph D_nP_n consists of a central core with five edges and four branches (see Figures 4 and 5). To analyze the structure of the dendrimer D_nP_n, we consider the following:

(i) The central core of D_nP_n has 5 edges.

(ii) Each of the four branches in D_nP_n has $2^{m-2} \times 96 - 4$ vertices, as derived in Lemma 5.

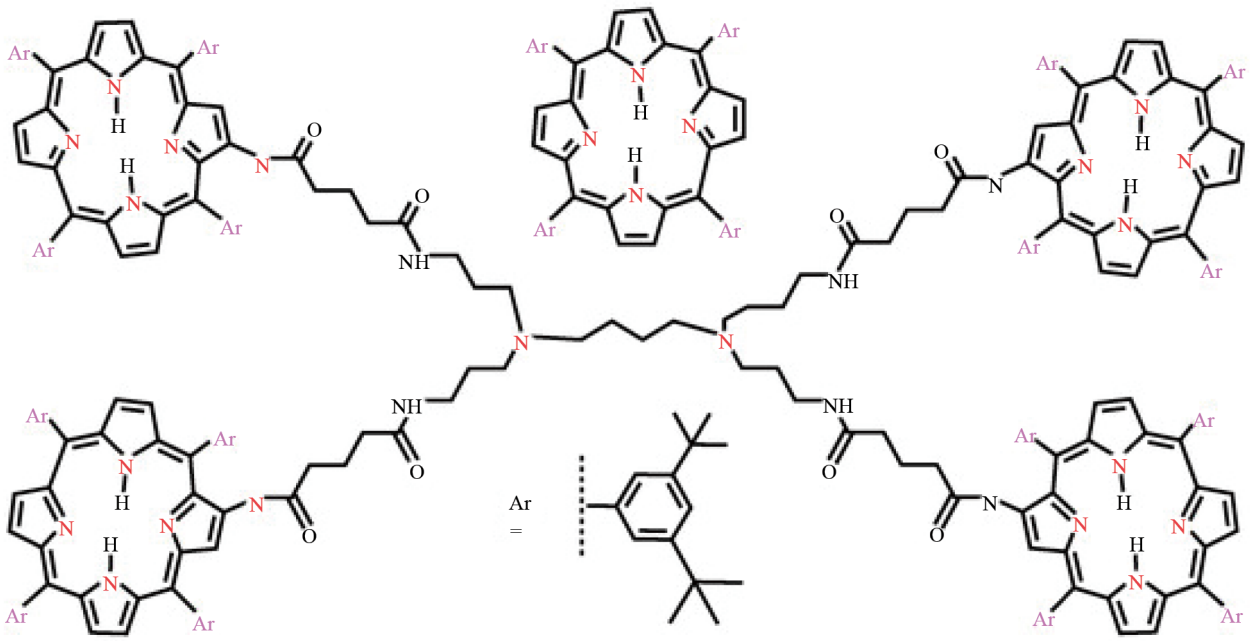

Figure 4. Molecular graph of porphyrin dendrimer D_4P_4 [45]

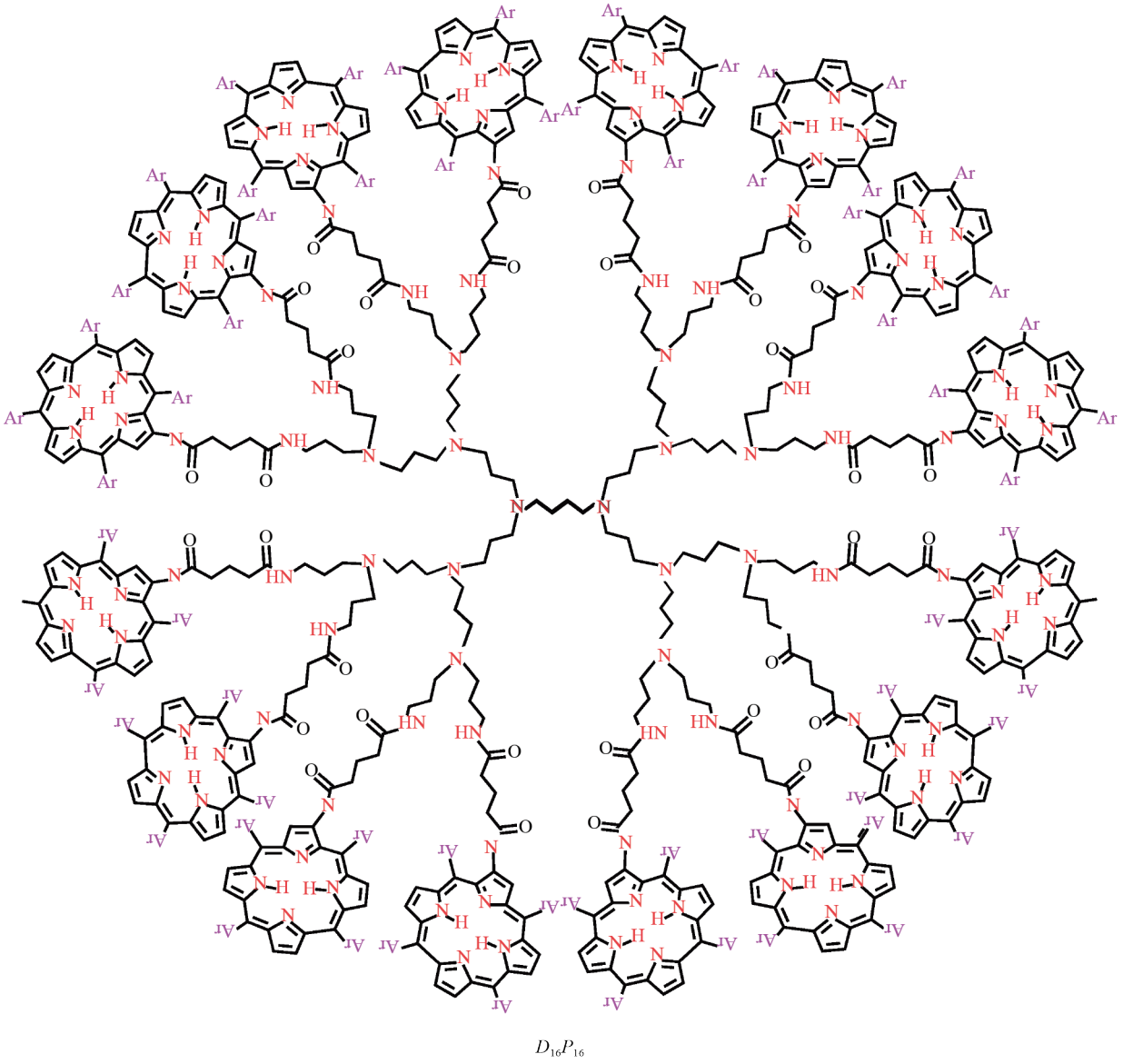

$D_{16}P_{16}$

Figure 5. Molecular graph of $D_{16}P_{16}$ dendrimer [45]

Subsequently, we determine the number of vertices with specific neighborhood multiple degrees using Definition 1. Then we obtain that: the vertices with neighborhood multiple degrees of 4 is

$$\xi_4 = 1 \times \left(\sum_{k=0}^{m-2} 2^k \right) + 2^{m-2} \times 28 = 2^{m-2} \times 30 - 1, \tag{46}$$

the vertices with neighborhood multiple degrees of 6 is

$$\xi_6 = 2 \times \left(\sum_{k=0}^{m-2} 2^k \right) + 2^{m-2} \times 8 = 2^{m-2} \times 12 - 2, \tag{47}$$

the vertices with neighborhood multiple degrees of 8 is

$$\xi_8 = 3, \tag{48}$$

the vertices with neighborhood multiple degrees of 9 is

$$\xi_9 = 2^{m-2} \times 18, \tag{49}$$

the vertices with neighborhood multiple degrees of 16 is

$$\xi_{16} = 2^{m-2} \times 8, \tag{50}$$

the vertices with neighborhood multiple degrees of 12 is

$$\xi_{12} = 2^{m-2} \times 12, \tag{51}$$

the vertices with neighborhood multiple degrees of 18 is

$$\xi_{18} = 2^{m-2}, \tag{52}$$

the vertices with neighborhood multiple degrees of 27 is:

$$\xi_{27} = 2^{m-2} \times 4, \tag{53}$$

and the remaining vertices with neighborhood multiple degrees of 3 are given by

$$\xi_3 = \left(2^{m-2} \times 96 - 4\right) - \left(2^{m-2} \times 85\right) = 2^{m-2} \times 11 - 4. \tag{54}$$

Additionally, the central core comprises 4 vertices. Such that:
(i) 2 vertices have neighborhood multiple degrees of 6.
(ii) 2 vertices have neighborhood multiple degrees of 4.
Thus, the total number of vertices $|V(\mathfrak{H})|$ in the molecular graph D_nP_n is:

$$|V(\mathfrak{H})| = 96 \times 2^m - 10. \tag{55}$$

Furthermore, among these vertices:
(i) 26×2^m vertices have a degree of 1.
(ii) $34 \times 2^m - 8$ vertices have a degree of 2.

(iii) $28 \times 2^m - 2$ vertices have a degree of 3.
(iv) 8×2^m vertices have a degree of 4.
Therefore, by Lemma 1 the total number of edges $|E(\mathfrak{H})|$ in the molecular graph D_nP_n is:

$$|E(\mathfrak{H})| = 105 \times 2^m - 11. \tag{56}$$

Lemma 5 Let $\mathfrak{G}$ be a $D_{16}P_{16}$ dendrimer with 4 branches. Then each branch has a total number of $2^{m-2} \times 96 - 4$ vertices.

Proof. Consider a molecular graph of $D_{16}P_{16}$ dendrimer. As it shown from (refer Figure 5), then

$$4 \times \left(\sum_{k=0}^{n-2} 2^k \right) + 2^{m-1} \times 44 = 4 \times \left(2^0 + 2^1 + 2^2 + \ldots + 2^{n-2}\right) + 2^{m-1} \times 44$$

$$= 2^m \times 24 - 4$$

$$= 2^{m-2} \times 96 - 4.$$

□

Next, the neighborhood multiple degrees of the end vertices for each edge are partitioned according to Definition 2, and the corresponding edge counts are presented in the Table 3 below.

Table 3. Edge set partition of the D_nP_n dendrimer via neighborhood multiple degrees of end-vertices of every edge

$\xi_u, \xi_v : uv \in E(\mathfrak{G})$	No. of edges
(3, 4)	$26n$
(3, 16)	$8n$
(4, 4)	$n+1$
(4, 6)	$9n-6$
(4, 9)	n
(6, 6)	$3n$
(6, 8)	$3n-6$
(6, 12)	$6n$
(9, 12)	$18n$
(9, 16)	$16n$
(9, 18)	n
(12, 18)	n
(12, 27)	$11n$
(18, 27)	n

Theorem 3 Let $\mathfrak{G}$ be a molecular graph of D_nP_n dendrimer, then
(i) $\Gamma_M ABC(\mathfrak{G}) = 54.128n - 5.851$.

(ii) $\Gamma_M GA(\mathfrak{G}) = 100.166n - 10.817$.
(iii) $\Gamma_M M_1(\mathfrak{G}) = 1{,}780n - 143$.
(iv) $\Gamma_M M_2(\mathfrak{G}) = 10{,}324n - 416$.
(v) $\Gamma_M R(\mathfrak{G}) = 16.422n - 1.840$.
(vi) $\Gamma_M F(\mathfrak{G}) = 25{,}734n - 880$.

Proof. We establish the proof using Table 3:
(i) Derived from equation (1), we obtain

$$\begin{aligned}\Gamma_M ABC(\mathfrak{G}) = {} & 26n\sqrt{\frac{3+4-2}{3\times 4}} + 8n\sqrt{\frac{3+16-2}{3\times 16}} + (n+1)\sqrt{\frac{4+4-2}{4\times 4}} + (9n-12)\sqrt{\frac{4+6-2}{4\times 6}} + n\sqrt{\frac{4+9-2}{4\times 9}} \\ & + 3n\sqrt{\frac{6+6-2}{6\times 6}} + (3n-6)\sqrt{\frac{6+8-2}{6\times 8}} + 18n\sqrt{\frac{9+12-2}{9\times 12}} + 16n\sqrt{\frac{9+16-2}{9\times 16}} + n\sqrt{\frac{9+18-2}{9\times 18}} \\ & + 6n\sqrt{\frac{6+12-2}{6\times 12}} + n\sqrt{\frac{12+18-2}{12\times 18}} + 11n\sqrt{\frac{12+27-2}{12\times 27}} + n\sqrt{\frac{18+27-2}{18\times 27}}. \end{aligned} \tag{57}$$

After simplifying (57) further, we get

$$\Gamma_M ABC(\mathfrak{G}) = 54.128n - 5.851. \tag{58}$$

□

(ii) From (2), we get

$$\begin{aligned}\Gamma_M GA(\mathfrak{G}) = {} & 26n\frac{2\sqrt{3\times 4}}{3+4} + 8n\frac{2\sqrt{3\times 16}}{3+16} + (n+1)\frac{2\sqrt{4\times 4}}{4+4} + (9n-6)\frac{2\sqrt{4\times 6}}{4+6} + n\frac{2\sqrt{4\times 9}}{4+9} \\ & + 3n\frac{2\sqrt{6\times 6}}{6+6} + (3n-6)\frac{2\sqrt{6\times 8}}{6+8} + 6n\frac{2\sqrt{6\times 12}}{6+12} + 18n\frac{2\sqrt{9\times 12}}{9+12} + 16n\frac{2\sqrt{9\times 16}}{9+16} \\ & + n\frac{2\sqrt{9\times 18}}{9+18} + n\frac{2\sqrt{12\times 18}}{12+18} + 11n\frac{2\sqrt{12\times 27}}{12+27} + n\frac{2\sqrt{18\times 27}}{18+27} \\ = {} & 100.166n - 10.817. \end{aligned} \tag{59}$$

(iii) From (3), we get

$$\Gamma_M M_1(\mathfrak{G}) = 26n(3+4) + 8n(3+16) + (n+1)(4+4) + (9n-6)(4+6) + n(4+9)$$
$$+ 3n(6+6) + (3n-6)(6+8) + 6n(6+12) + 18n(9+12)$$
$$+ 16n(9+16) + n(9+18) + n(12+18)$$
$$+ 11n(12+27) + n(18+27). \tag{60}$$

After simplifying (60) further, we obtain

$$\Gamma_M M_1(\mathfrak{G}) = 1{,}780n - 143. \tag{61}$$

(iv) From (4), we get

$$\Gamma_M M_2(\mathfrak{G}) = 26n(3\times 4) + 8n(3\times 16) + (n+1)(4\times 4) + (9n-6)(4\times 6) + n(4\times 9) + 3n(6\times 6)$$
$$+ (3n-6)(6\times 8) + 6n(6\times 12) + 18n(9\times 12) + 16n(9\times 12) + n(9\times 18)$$
$$+ n(12\times 18) + 11n(12\times 27) + n(18\times 27). \tag{62}$$

After simplifying (62) further, we get

$$\Gamma_M M_2(\mathfrak{G}) = 10{,}324n - 416. \tag{63}$$

(v) From (5), we get

$$\Gamma_M R(\mathfrak{G}) = 26n\frac{1}{\sqrt{3\times 4}} + 8n\frac{1}{\sqrt{3\times 16}} + (n+1)\frac{1}{\sqrt{4\times 4}} + (9n-6)\frac{1}{\sqrt{4\times 16}}$$
$$+ n\frac{1}{\sqrt{4\times 9}} + 3n\frac{1}{\sqrt{6\times 6}} + (3n-6)\frac{1}{\sqrt{6\times 8}} + 6n\frac{1}{\sqrt{6\times 12}}$$
$$+ 18n\frac{1}{\sqrt{9\times 12}} + 16n\frac{1}{\sqrt{9\times 16}} + n\frac{1}{\sqrt{9\times 18}} + n\frac{1}{\sqrt{12\times 18}}$$
$$+ 11n\frac{1}{\sqrt{12\times 27}} + n\frac{1}{\sqrt{18\times 27}}. \tag{64}$$

After simplifying (64) further, we find

$$\Gamma_M R(\mathfrak{G}) = 16.422n - 1.840. \tag{65}$$

(vi) From (6), we get

$$\begin{aligned}\Gamma_M F(\mathfrak{G}) = {} & 26n(3^2+4^2)+8n(3^2+16^2)+(n+1)(4^2+4^2)+(9n-6)(4^2+6^2)+n(4^2+9^2)\\ & +3n(6^2+6^2)+(3n-6)(6^2+8^2)+6n(6^2+12^2)+18n(9^2+12^2)+16n(9^2+16^2)\\ & +n(9^2+18^2)+n(12^2+18^2)+11n(12^2+27^2)+n(18^2+27^2).\end{aligned} \tag{66}$$

After simplifying (66) further, we get

$$\Gamma_M F(\mathfrak{G}) = 25{,}934n - 880. \tag{67}$$

5. Graphical visualization of neighborhood multiple TIs across dendrimer generations

In this section, we present a graphical visualization of the neighborhood multiple TIs for various dendrimers (PETIM, DPZ_n, and P_nP_n). Additionally, we discuss the performance of neighborhood multiple TIs in dendrimer generation analysis.

PETIM: The neighborhood multiple TIs computed from a PETIM dendrimer up to generation 5 reveal distinct growth patterns across the different TIs. As the number of generations increases, all TIs exhibit an exponential increase in their values. Notably, $\Gamma_M F(\mathfrak{G})$ and $\Gamma_M M_2(\mathfrak{G})$ TIs exhibit a strong exponential increase with each generation, indicating their sensitivity to the increasing structural complexity of the dendrimer. The other TIs, such as $\Gamma_M M_1(\mathfrak{G})$, $\Gamma_M GA(\mathfrak{G})$, and $\Gamma_M ABC(\mathfrak{G})$, demonstrate more moderate, linear growth, reflecting a steadier response to generational changes. This suggests that as the PETIM dendrimer expands, certain TIs capture complex branching and connectivity patterns more distinctly, while others respond in a more restrained and linear manner, as shown in Figure 6.

***DPZn*:** The plotted neighborhood multiple degree-based TIs of the Zinc porphyrin dendrimer exhibit varying growth behaviors as the generation number n increases. TIs such as $\Gamma_M F(\mathfrak{G})$ and $\Gamma_M M_2(\mathfrak{G})$ display exponential growth, driven by their large multiplicative factors and the exponential term 2^n. This rapid increase highlights their sensitivity to the dendrimer's structural complexity as the generation expands. In contrast, TIs like $\Gamma_M ABC(\mathfrak{G})$ and $\Gamma_M R(\mathfrak{G})$ exhibit more linear or moderate growth patterns, indicating a more restrained response to the structural changes in the dendrimer. The linearity in these TIs suggests they capture less complex or more localized topological features, making them less responsive to the exponential expansion of the dendrimer's structure, as illustrated in Figure 7.

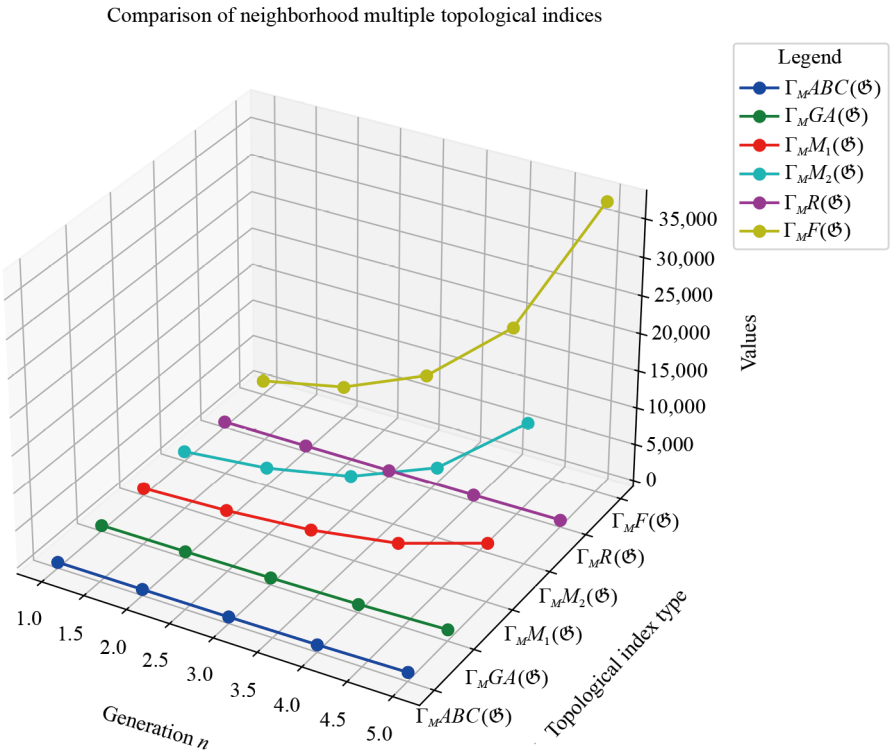

Figure 6. Numerical visualization of neighbourhood multiple TIs of PETIM dendrimer

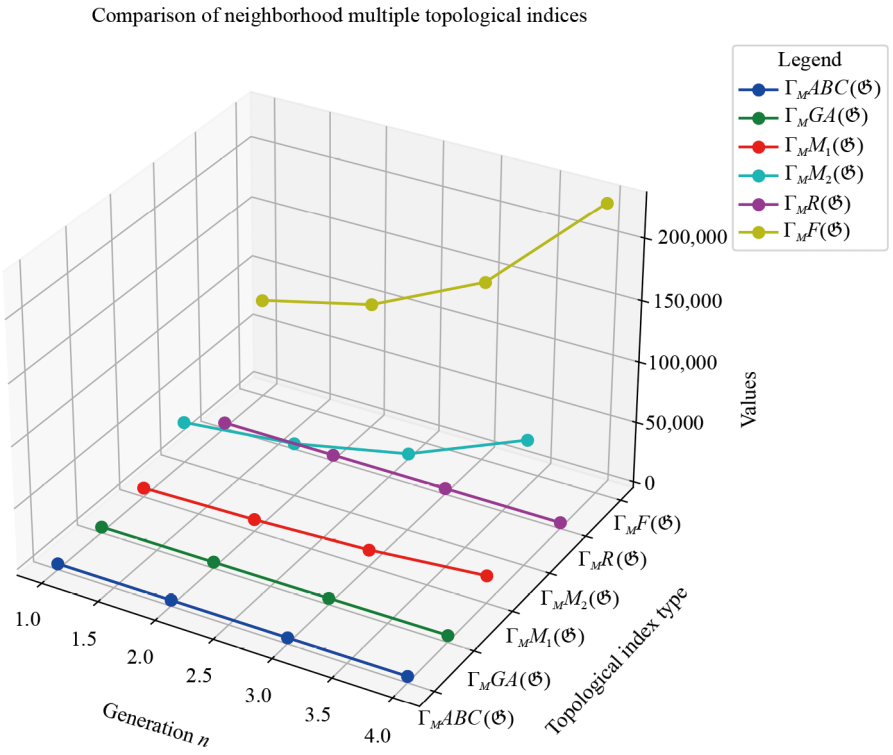

Figure 7. Numerical visualization of neighborhood multiple TIs of DPZ_n dendrimer

***DnPn*:** The graphs of the neighborhood multiple TIs for the porphyrin dendrimer (D_nP_n) reveal a clear linear relationship between the generation number n and the computed index values. As n increases, all TIs ($\Gamma_M ABC(\mathfrak{G})$, $\Gamma_M GA(\mathfrak{G})$, $\Gamma_M M_1(\mathfrak{G})$, $\Gamma_M M_2(\mathfrak{G})$, $\Gamma_M R(\mathfrak{G})$, and $\Gamma_M F(\mathfrak{G})$) exhibit a consistent linear growth, indicating that the complexity of the dendrimer structure expands predictably with each new generation. Notably, the TIs $\Gamma_M M_2(\mathfrak{G})$ and $\Gamma_M F(\mathfrak{G})$ increase more rapidly compared to the others, suggesting that these TIs are particularly sensitive to the structural growth of the dendrimer. In contrast, TIs like $\Gamma_M M_1(\mathfrak{G})$ and $\Gamma_M M_2(\mathfrak{G})$ reach significantly higher values for larger generations, highlighting their strong dependence on the dendrimer's size and complexity. Overall, the consistent upward trends across all TIs underscore the predictable and structured growth of the porphyrin dendrimer, as illustrated in Figure 8, providing valuable insights into its evolving properties as it increases in generations.

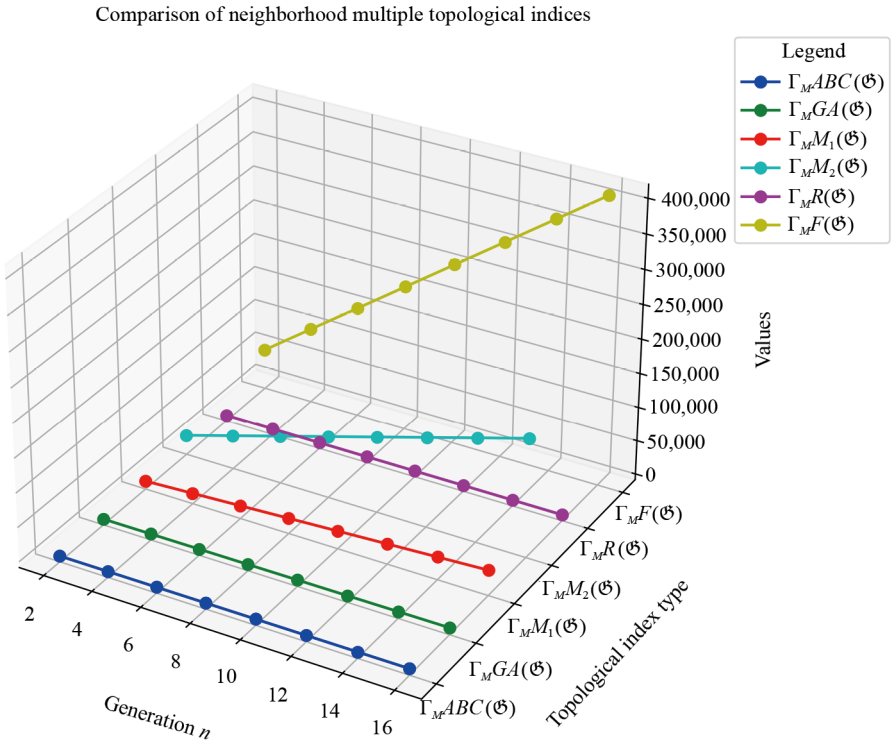

Figure 8. Numerical visualization of neighbourhood multiple TIs of $D_{16}P_{16}$ dendrimer

5.1 *Performance of neighborhood multiple TIs in dendrimers generation analysis*

The neighborhood multiple degree-based TIs computed for the PETIM dendrimer, porphyrin dendrimer (D_nP_n), and Zinc porphyrin dendrimer $(DPZn)$ reveal distinct growth patterns closely aligned with the structural expansion of these dendrimers across generations. For the PETIM dendrimer, exponential growth is observed in all TIs, particularly $\Gamma_M F(\mathfrak{H})$ and $\Gamma_M M_2(\mathfrak{H})$, underscoring their high sensitivity to increasing structural complexity. In contrast, the porphyrin dendrimer exhibits consistent linear growth across all TIs, with $\Gamma_M M_2(\mathfrak{H})$ and $\Gamma_M F(\mathfrak{H})$ showing slightly steeper increases. The Zinc porphyrin dendrimer displays exponential growth in $\Gamma_M F(\mathfrak{H})$ and $\Gamma_M M_2(\mathfrak{H})$, while other TIs, such as $\Gamma_M ABC(\mathfrak{H})$ and $\Gamma_M R(\mathfrak{H})$, follow more moderate, linear trends.

The exponential growth observed in TIs like $\Gamma_M F(\mathfrak{H})$ and $\Gamma_M M_2(\mathfrak{H})$ across all three dendrimer types highlights the responsiveness of these TIs to increasing structural complexity. This suggests that these TIs are particularly effective at capturing the complex branching and connectivity patterns that develop as dendrimers grow. Conversely, the linear growth trends in TIs such as $\Gamma_M M_1(\mathfrak{H})$, $\Gamma_M GA(\mathfrak{H})$, and $\Gamma_M ABC(\mathfrak{H})$ suggest that these TIs are more reflective of overall size rather

than local structural complexities. These findings underscore the varied sensitivity of different TIs to changes in dendrimer structure, providing a nuanced understanding of how dendrimer complexity can be quantified using neighborhood multiple degree-based TIs.

6. Result discussion and conclusion

The results of this study provide a detailed examination of six neighborhood multiple TIs for dendrimers, highlighting their distinct growth patterns across different dendrimer types and generations. Specifically, PETIM dendrimers exhibit exponential growth in all TIs, with indices such as $\Gamma_M F(\mathfrak{G})$ and $\Gamma_M M_2(\mathfrak{G})$ demonstrating exceptional sensitivity to structural complexity. In contrast, porphyrin dendrimers (D_nP_n) display linear growth across all indices, reflecting a consistent structural expansion with generational increases. Zinc porphyrin dendrimers (DPZ_n) exhibit a combination of exponential growth in TIs like $\Gamma_M F(\mathfrak{G})$ and $\Gamma_M M_2(\mathfrak{G})$, and seemingly linear trends in TIs such as $\Gamma_M ABC(\mathfrak{G})$, $\Gamma_M GA(\mathfrak{G})$ and $\Gamma_M R(\mathfrak{G})$, likely due to the slower growth rate of these TIs.

The contrasting behaviors among these TIs underscore their varied sensitivity to the complex topological and branching patterns of dendrimers. Exponentially growing indices, particularly $\Gamma_M F(\mathfrak{G})$ and $\Gamma_M M_2(\mathfrak{G})$, effectively capture the hierarchical complexity of dendrimers with extensive branching or layered structures. In contrast, TIs with linear trends provide a more generalized representation of dendrimer size and connectivity. These findings emphasize the utility of neighborhood multiple TIs in comprehensively characterizing dendrimer structures and their growth dynamics. It is important to note that, only three dendrimer types (PETIM, D_nP_n, and DPZ_n) were analyzed. Incorporating our proposed methodology to dendrimers of other families with varying branching factors could enhance the generalizability of the results and efficiency of our method. Additionally, our analysis was restricted to generations from $n = 1$ to 5 for PETIM, $n = 1$ to 4 for DPZ_n, and $n = 2$ to 16 for D_nP_n. Extending this range could reveal additional growth behaviors or deviations in larger generations. In conclusion, future studies could perform QSPR model analysis to predict the properties of these dendrimers and complex structures of other types such as nano structures and graphenes to establish the predictive capability of our method.

Conflict of interest

The authors declare no competing financial interest.

References

[1] Buhleier E, Wehner W, Vögtle F. "Cascade"- and "nonskid-chain-like" syntheses of molecular cavity topologies. *Synthesis*. 1978; 2: 155-158. Available from: https://doi.org/10.1055/s-1978-24702.

[2] Mittal P, Saharan A, Verma R, Altalbawy F, Alfaidi MA, Batiha GES, et al. Dendrimers: a new race of pharmaceutical nanocarriers. *BioMed Research International*. 2021. Available from: https://doi.org/10.1155/2021/8844030.

[3] Ethirajan M, Chen Y, Joshi P, Pandey RK. The role of porphyrin chemistry in tumor imaging and photodynamic therapy. *Chemical Society Reviews*. 2011; 40(1): 340-362. Available from: https://doi.org/10.1039/B915149B.

[4] Rouvray D. The pioneering contributions of Cayley and Sylvester to the mathematical description of chemical structure. *Journal of Molecular Structure: THEOCHEM*. 1989; 185: 1-14. Available from: https://doi.org/10.1016/0166-1280(89)85003-1.

[5] Natarajan R, Kamalakanan P, Nirdosh I. Applications of topological indices to structure-activity relationship modeling and selection of mineral collectors. *Indian Journal of Chemistry-Section A*. 2003; 42(6): 1330-1346.

[6] Wiener H. Structural determination of paraffin boiling points. *Journal of the American Chemical Society*. 1947; 69(1): 17-20. Available from: https://doi.org/10.1021/ja01193a005.

[7] Gutman I, Trinajstić N. Graph theory and molecular orbitals. Total φ-electron energy of alternant hydrocarbons. *Chemical Physics Letters*. 1972; 17(4): 535-538. Available from: https://doi.org/10.1016/0009-2614(72)85099-1.

[8] Furtula B, Gutman I. A forgotten topological index. *Journal of Mathematical Chemistry*. 2015; 53(4): 1184-1190. Available from: https://doi.org/10.1007/s10910-015-0480-z.

[9] Randic M. Characterization of molecular branching. *Journal of the American Chemical Society*. 1975; 97(23): 6609-6615. Available from: https://doi.org/10.1021/ja00856a001.

[10] Estrada E, Torres L, Rodriguez L, Gutman I. An atom-bond connectivity index: modelling the enthalpy of formation of alkanes. *Indian Journal of Chemistry*. 1998; 37A: 849-855.

[11] Ghorbani M, Hosseinzadeh MA. Computing ABC4 index of nanostar dendrimers. *Optoelectronics and Advanced Materials-Rapid Communications*. 2010; 4: 1419-1422.

[12] Vukičević D, Furtula B. Topological index based on the ratios of geometrical and arithmetical means of end-vertex degrees of edges. *Journal of Mathematical Chemistry*. 2009; 46: 1369-1376. Available from: https://doi.org/10.1007/s10910-009-9520-x.

[13] Aslam A, Jamil MK, Gao W, Nazeer W. Topological aspects of some dendrimer structures. *Nanotechnology Reviews*. 2018; 7(2): 123-129. Available from: https://doi.org/10.1515/ntrev-2017-0184.

[14] Graovac A, Ghorbani M, Hosseinzadeh MA. Computing fifth geometric-arithmetic index for nanostar dendrimers. *Journal of Discrete Mathematics and Its Applications*. 2011; 1(1-2): 33-42.

[15] Bača M, Horváthová J, Mokrišová M, Suhányiová A. On topological indices of fullerenes. *Applied Mathematics and Computation*. 2015; 251: 154-161. Available from: https://doi.org/10.1016/j.amc.2014.11.069.

[16] Gao W, Wang W. The fifth geometric-arithmetic index of bridge graph and carbon nanocones. *Journal of Difference Equations and Applications*. 2017; 23(1-2): 100-109. Available from: https://doi.org/10.1080/10236198.2016.1197214.

[17] Gao W, Wang W, Jamil MK, Farahani MR. Electron energy studying of molecular structures via forgotten topological index computation. *Journal of Chemistry*. 2016. Available from: https://doi.org/10.1155/2016/1053183.

[18] Gao W, Siddiqui MK, Naeem M, Imran M. Computing multiple ABC index and multiple GA index of some grid graphs. *Open Physics*. 2018; 16: 588-598. Available from: https://doi.org/10.1515/phys-2018-0077.

[19] Zaman S, Ullah A, Shafaqat A. Structural modeling and topological characterization of three kinds of dendrimer networks. *The European Physical Journal E*. 2023; 46(5): 36. Available from: https://doi.org/10.1140/epje/s10189-023-00297-4.

[20] Zaman S, Ahmed W, Sakeena A, Rasool KB, Ashebo MA. Mathematical modeling and topological graph description of dominating David derived networks based on edge partitions. *Scientific Reports*. 2023; 13(1): 15159. Available from: https://doi.org/10.1038/s41598-023-42340-6.

[21] Liaqat S, Mufti ZS, Shang Y. Newly defined fuzzy Misbalance Prodeg Index with application in multi-criteria decision-making. *AIMS Mathematics*. 2024; 9(8): 20193-20220. Available from: https://doi.org/10.3934/math.2024984.

[22] Noureen S, Batool R, Albalahi AM, Shang Y, Alraqad T, Ali A. On tricyclic graphs with maximum atom-bond sum-connectivity index. *Heliyon*. 2024; 10(14): e33841. Available from: https://doi.org/10.1016/j.heliyon.2024.e33841.

[23] Ali A, Shang Y, Dimitrov D, Réti T. Ad-Hoc Lanzhou index. *Mathematics*. 2023; 11(20): 4256. Available from: https://doi.org/10.3390/math11204256.

[24] Gowtham KJ. New vertex-edge sombor, Nirmala and Misbalance Indices. *TWMS Journal of Applied and Engineering Mathematics*. 2024; 14(2): 597-604.

[25] Gowtham KJ, Narahari N. The study of line graphs of subdivision graphs of some rooted product graphs via K-Banhatti indices. *International Journal of Mathematics for Industry*. 2023; 15(01): 2350003. Available from: https://doi.org/10.1142/S266133522350003X.

[26] Mondal S, De N, Pal A. On some new neighbourhood degree based indices. *arXiv:190611215*. 2019. Available from: https://doi.org/10.48550/arXiv.1906.11215.

[27] Mondal S, Siddiqui MK, De N, Pal A. Neighborhood M-polynomial of crystallographic structures. *Biointerface Research in Applied Chemistry*. 2021; 11(2): 9372-9381. Available from: https://doi.org/10.33263/BRIAC112.93729381.

[28] Abubakar MS, Aremu KO, Aphane M. Neighborhood versions of geometric-arithmetic and atom bond connectivity indices of some popular graphs and their properties. *Axioms*. 2022; 11(9): 487. Available from: https://doi.org/10.3390/axioms11090487.

[29] Ullah A, Qasim M, Zaman S, Khan A. Computational and comparative aspects of two carbon nanosheets with respect to some novel topological indices. *Ain Shams Engineering Journal*. 2022; 13(4): 101672. Available from: https://doi.org/10.1016/j.asej.2021.101672.

[30] Abubakar MS, Aremu KO, Aphane M, Amusa LB. A QSPR analysis of physical properties of antituberculosis drugs using neighbourhood degree-based topological indices and support vector regression. *Heliyon*. 2024; 10(7): e28260. Available from: https://doi.org/10.1016/j.heliyon.2024.e28260.

[31] Abubakar MS, Ejima O, Sanusi RA, Ibrahim AH, Aremu KO. Predicting antibacterial drugs properties using graph topological indices and machine learning. *IEEE Access*. 2024; 12: 181420-181435. Available from: https://doi.org/10.1109/ACCESS.2024.3503760.

[32] Ejima O, Abubakar MS, Pawa SSS, Ibrahim AH, Aremu KO. Ensemble learning and graph topological indices for predicting physical properties of mental disorder drugs. *Physica Scripta*. 2024; 99(10): 106009. Available from: https://doi.org/10.1088/1402-4896/ad79a4.

[33] Imran M, Bokhary S, Manzoor S, Siddiqui MK. On molecular topological descriptors of certain families of nanostar dendrimers. *Eurasian Chemical Communications*. 2020; 2(6): 680-687. Available from: https://doi.org/10.33945/SAMI/ECC.2020.6.5.

[34] Krishnasamy TR, Angamuthu M. Neighborhood-based descriptors for porphyrin dendrimers. *Biointerface Research in Applied Chemistry*. 2021; 12(5): 6297-6307. Available from: https://doi.org/10.33263/BRIAC125.62976307.

[35] Jones DE, Ghandehari H, Facelli JC. Predicting cytotoxicity of PAMAM dendrimers using molecular descriptors. *Beilstein Journal of Nanotechnology*. 2015; 6(1): 1886-1896. Available from: https://doi.org/10.3762/bjnano.6.192.

[36] Bokhary SAUH, Imran M, Manzoor S. On molecular topological properties of dendrimers. *Canadian Journal of Chemistry*. 2016; 94(2): 120-125. Available from: https://doi.org/10.1139/cjc-2015-0466.

[37] Mondal S, De N, Pal A. Neighborhood degree sum-based molecular descriptors of fractal and Cayley tree dendrimers. *The European Physical Journal Plus*. 2021; 136(3): 1-37. Available from: https://doi.org/10.1140/epjp/s13360-021-01292-4.

[38] Kulli V. Neighborhood sum atom bond connectivity indices of some nanostar dendrimers. *International Journal of Mathematics and Computer Research*. 2023; 11(2): 3230-3235. Available from: https://doi.org/10.47191/ijmcr/v11i2.01.

[39] Sarkar P, De N, Pal A. On some neighborhood degree-based multiplicative topological indices and their applications. *Polycyclic Aromatic Compounds*. 2022; 42(10): 7738-7753. Available from: https://doi.org/10.1080/10406638.2021.2007141.

[40] Fahad A, Qureshi MI, Noureen S, Iqbal Z, Zafar A, Ishaq M. Topological descriptors of poly propyl ether imine (PETIM) dendrimers. *Biointerface Research in Applied Chemistry*. 2021; 11(3): 10968-10978. Available from: https://doi.org/10.33263/BRIACI13.1096810978.

[41] Bashir Y, Aslam A, Kamran M, Qureshi MI, Jahangir A, Rafiq M, et al. On forgotten topological indices of some dendrimers structure. *Molecules*. 2017; 22(6): 867. Available from: https://doi.org/10.3390/molecules22060867.

[42] Abubakar MS, Aremu KO, Aphane M, Siddiqui MK. Exploring topological indices of oligothiophene dendrimer via neighbourhood M-polynomial. *RAIRO-Operations Research*. 2025; 59(1): 149-161. Available from: https://doi.org/10.1051/ro/2024138.

[43] Aslam A, Bashir Y, Ahmad S, Gao W. On topological indices of certain dendrimer structures. *Zeitschrift für Naturforschung A*. 2017; 72(6): 559-566. Available from: https://doi.org/10.1515/zna-2017-0081.

[44] Aslam A, Ahmad S, Gao W. On certain topological indices of boron triangular nanotubes. *Zeitschrift für Naturforschung A*. 2017; 72(8): 711-716. Available from: https://doi.org/10.1515/zna-2017-0135.

[45] Ali Y, Bibi Z, Kiran Q. Forgotten coindex of some non-toxic dendrimers structure used in targeted drug delivery. *Main Group Metal Chemistry*. 2021; 44(1): 22-31. Available from: https://doi.org/10.1515/mgmc-2021-0004.